PHYSICAL REVIEW D **84,** 085002 (2011)

Confluent Heun functions in gauge theories on thick braneworlds

M. S. Cunha[1] and H. R. Christiansen[1,2]

[1]*Grupo de Física Teórica, State University of Ceara (UECE), Avenida Paranjana 1700, 60740-903 Fortaleza, Ceará, Brazil*
[2]*Universidade Estadual Vale do Acaraú, Avenida da Universidade 850, 62040-370 Sobral, Ceará, Brazil*

(Received 15 June 2011; published 3 October 2011)

We investigate the propagation modes of gauge fields in an infinite Randall-Sundrum scenario. In this model a sine-Gordon soliton represents our *thick* four-dimensional braneworld while an exponentially coupled scalar acts for the dilaton field. For the gauge-field motion we find a differential equation which can be transformed into a confluent Heun equation. By means of another change of variables we obtain a related Schrödinger equation with a family of symmetric rational $(\gamma - \omega z^2)/(1 - z^2)^2$ potential functions. We discuss both results and present the infinite spectrum of analytical solutions for the gauge field. Finally, we assess the existence and the relative weights of Kaluza-Klein modes in the present setup.

DOI: 10.1103/PhysRevD.84.085002 PACS numbers: 11.10.Kk, 04.50.−h

I. INTRODUCTION

One of the main purposes of superstring theory is the inclusion of all the relevant fields of nature together in one single Lagrangian. Field-theoretic scenarios inspired in such a theory put in contact gauge and matter fields with metric degrees of freedom, altogether defined in some extra-dimensional space [1]. Extra dimensions, combined with the influence of the gravitational field, modify nontrivially all sectors so that gauge forces must be proven to remain the same in the usual four-dimensional (4D) subspace or predict new physics in some consistent way. Localization in the gauge sector is expected to hold and the effective 4D electromagnetic force must be mediated by massless photons as usual. On the other hand, higher-dimensional spaces help solving fundamental problems such as the hierarchy gap between the Planck scale and gauge coupling constants in the standard model [2].

Also inspired in string theory is the use of branes to represent our Universe. In string theory, gauge modes are deposited on D-branes from open strings ending on them, so we expect gauge fields in field-theoretic models to have finite localized modes on stringy topological defects of lower dimensionality. Actually, to obtain finite eigenstates in 4D it has been shown that to fulfill this task we need not just gravity but also a dilaton [3,4], a field already predicted in string theory.

In the present paper, we describe gauge fields in a warped five-dimensional bulk with a dilaton and a brane defect that mimics the ordinary world. Both brane and dilaton configurations are geometrically consistent solutions of a two scalar world action in a curved 5D space-time where the field potential is of sine-Gordon type.

We show a relationship between the fundamental parameters of the 5D theory which is crucial to determine the dynamics of the fields both in the bulk and ordinary space. Indeed, for different choices of a parameter defined by the quotient of some power of the sine-Gordon frequency amplitude and the 5D Planck mass, the equations of motion of the gauge field can be completely different. Notably, in Ref. [5] we have been able to find the whole spectrum of a theory involving both Maxwell and Kalb-Ramond fields for a particular value of this parameter. As we will see, there exists a minimal value for the dilaton coupling constant above which the finiteness of the action is assured and it is directly related to the localization of gauge fields.

In what follows we analytically obtain the propagation modes (massless and massive) of a gauge theory in a background of the sine-Gordon type that results in new equations of motion. We show that the dynamics of the quantum-mechanical system associated with the problem is given by a simple (rational) potential function and that the solutions to the Schrödinger equation are of the Mathieu type (with a power-law factor). In a more general case, we obtain the exact spectrum given by the set of confluent Heun functions and show that Kaluza-Klein (KK) states are strongly suppressed in ordinary space.

The paper is organized as follows. In the next section, we present the geometrical background. In Sec. III we introduce the action for the 5D gauge field coupled to warped gravity and a dilaton background and derive the 5D equations of motion. In Sec. IV we obtain the quantum analog problem showing explicitly the quantum-mechanical Schrödinger potential. The eigenvalue spectrum is computed and graphically shown. Next, in Secs. V and VI we discuss the general problem and draw our conclusions. Other recent results about thick braneworlds can be found in e.g. [6].

II. GEOMETRICAL BACKGROUND

Our framework is a five-dimensional space-time embedding a four-dimensional membrane also called thick brane. The (spacelike) extra dimension is assumed infinite and the brane will be dynamically obtained as a solution to the Einstein equations for gravity coupled to a pair of scalar fields. One of these scalars represents a domain wall defect (the thick brane) while the other is the dilaton. The dilaton,

together with the warping of the fifth dimension, happens to be crucial in the gauge theory that will be developed and makes more clear the stringy origin of the theory. Since gauge-field theory is conformal [7], all the information coming from the warping of the 4D metric is automatically lost. As a consequence, the photon is non-normalizable in the four-dimensional space unless the gauge coupling is dynamically modified. Indeed, the exponential coupling of both the dilaton and the 5D warping to the gauge field conveniently modifies the scaling properties and the zero mode becomes localized [3].

The five-dimensional world action which determines the background is

$$S_B = \int d^4x dy \sqrt{-\det G_{MN}} \times \left[2M^3 R - \frac{1}{2}(\partial\Phi)^2 - \frac{1}{2}(\partial\Pi)^2 - \mathcal{V}(\Phi, \Pi) \right], \quad (1)$$

where M is the Planck mass in 5D, and R is the Ricci scalar. The solution for Φ represents the world membrane and the corresponding field solution for Π will be the dilaton configuration consistent with the metric and the kink. As usual we adopt Latin capitals on the bulk and Greek lower case letters on 4D.

We next adopt the following ansatz for the metric:

$$ds^2 = e^{2A(y)} \eta_{\mu\nu} dx^\mu dx^\nu + e^{2\Sigma(y)} dy^2, \quad (2)$$

where Λ and Σ depend just on the fifth coordinate, y, and diag $(\eta) = (-1, 1, 1, 1)$. The equations of motion for Eq. (1) are

$$\begin{aligned} &\tfrac{1}{2}(\Phi')^2 + \tfrac{1}{2}(\Pi')^2 - e^{2\Sigma(y)} \mathcal{V}(\Phi, \Pi) = 24M^3(\Lambda')^2, \\ &\tfrac{1}{2}(\Phi')^2 + \tfrac{1}{2}(\Pi')^2 + e^{2\Sigma(y)} \mathcal{V}(\Phi, \Pi) \\ &\quad = -12M^3\Lambda'' - 24M^3(\Lambda')^2 + 12M^3\Lambda'\Sigma', \end{aligned} \quad (3)$$

and

$$\begin{aligned} \Phi'' + (4\Lambda' - \Sigma')\Phi' &= e^{2\Sigma} \frac{\partial \mathcal{V}}{\partial \Phi}, \\ \Pi'' + (4\Lambda' - \Sigma')\Pi' &= e^{2\Sigma} \frac{\partial \mathcal{V}}{\partial \Pi}, \end{aligned} \quad (4)$$

where the prime means derivative with respect to y.

By means of a supergravity motivated functional $\mathcal{W}(\Phi)$ defined by [8]

$$\Phi' = \frac{d\mathcal{W}}{d\Phi}, \quad (5)$$

the system of differential equations can be more easily handled. This method is also applicable to nonsupersymmetric domain walls [9,10] as the present one.

First, we consider the action in the absence of gravity (and no dilaton) in order to obtain an expression for Φ. Then, we put this solution into the equations of motion (3) and (4).

The standard sine-Gordon Lagrangian reads

$$L_{SG} = -\tfrac{1}{2}\partial^2\Phi - V(\Phi) \quad (6)$$

with

$$V(\Phi) = \frac{1}{b^2}(1 - \cos(b\Phi)).$$

The free parameter b signals bulk symmetries $\delta\Phi \to 2n\pi/b (n \in Z)$ among the vacua of this theory. Solutions interpolating vacua are possible and, assuming they depend only on y, one-solitons read

$$\Phi(y) = \frac{4}{b} \arctan e^y. \quad (7)$$

These functions kink on our 4D-world slice, namely, at $y \sim 0$.

In a gravitational background of the form (2), now including also the dilaton, the equations of motion (3) and (4) are still compatible with solutions (7) provided we find the appropriate potential functional $\mathcal{V}$ for the general action (1), viz.

$$\mathcal{V}(\Phi, \Pi) = \exp(\Pi/\sqrt{12M^3}) \left(\frac{1}{2} \left(\frac{d\mathcal{W}}{d\Phi} \right)^2 - \frac{5}{32M^3} \mathcal{W}(\Phi)^2 \right). \quad (8)$$

Taking into account Eq. (5), the superpotential functional results

$$\mathcal{W}(\Phi) = -\frac{4}{b^2} \cos\left(\frac{b}{2}\Phi \right) \quad (9)$$

and then

$$\mathcal{V}(\Phi, \Pi) = -e^{(\Pi/\sqrt{12M^3})} \left(\frac{4}{b^2} \sin^2 \frac{b}{2}\Phi + \frac{5}{2M^3 b^4} \cos^2 \frac{b}{2}\Phi \right). \quad (10)$$

If we now conveniently write the Hamiltonian à la Bogomol'nyi, we can detect the following relations among the warping functions, the dilaton and the superpotential

$$\Pi = -\sqrt{3M^3}\Lambda, \quad \Sigma = \Lambda/4, \quad \Lambda' = -\mathcal{W}/12M^3. \quad (11)$$

Finally, totally solving the equations of motion, the dilaton field is given by

$$\Pi(y) = \frac{1}{\sqrt{3M^3 b^2}} \ln \cosh y, \quad (12)$$

and

$$\Lambda = -\frac{1}{3M^3 b^2} \ln \cosh y, \quad \Sigma = -\frac{1}{12M^3 b^2} \ln \cosh y. \quad (13)$$

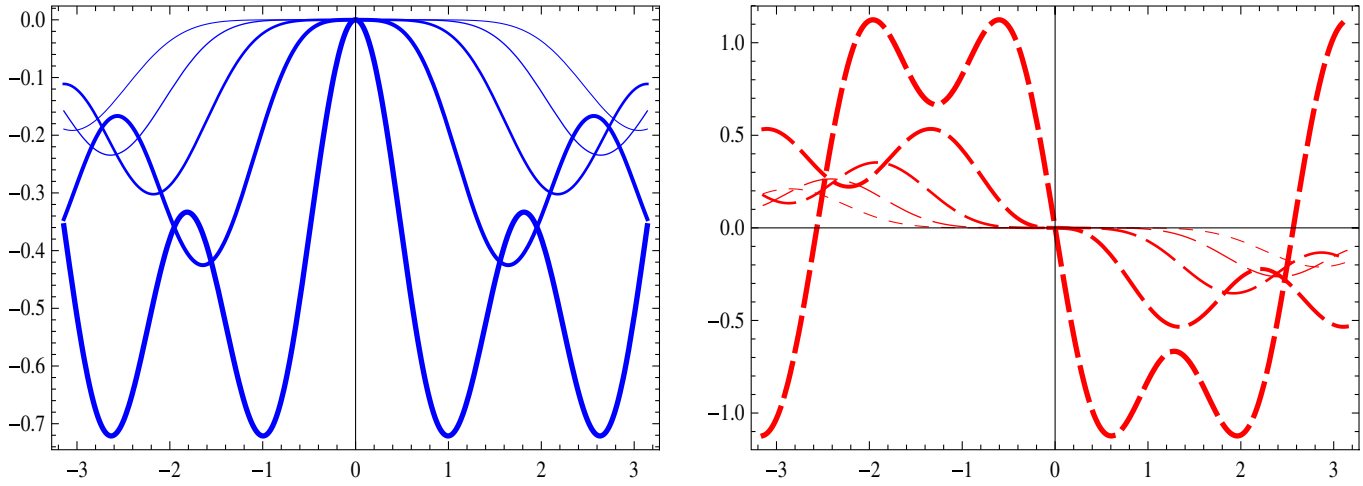

FIG. 1 (color online). Family of background potential functionals $\mathcal{V}(\Phi)$ [Eq. (14)] for different values of $a \equiv 1/6M^3b^2$: even $a = 2, 4, 6, 8, 10$ (solid line), odd $a = 1, 3, 5, 7, 9$ (dashed line). For clarity we adopted thinner lines for bigger values of a.

The relation between Π and Φ allows also writing $\mathcal{V}$ as

$$\mathcal{V}(\Phi) = -\frac{4}{b^2}\left(\sin\frac{b}{2}\Phi\right)^{1/6M^3b^2}\left(1+\left(\frac{5}{8M^3b^2}-1\right)\cos^2\frac{b}{2}\Phi\right), \tag{14}$$

which fully shows its dependence on b and M (see Fig. 1).

As it happens with dilaton configurations related to D-brane solutions, functions such as (7) and (12) are singular when $|y| \to \infty$. However, since the metric vanishes exponentially and both dilaton and warp factors operate under an exponential coupling, the model is kept free of divergences.

The warping functions amount to a shift in the effective four-dimensional Planck scale, which remains finite with the following definition:

$$M_P^2 \equiv M^3 \int_{-\infty}^{\infty} dy e^{4\Lambda(y)+\Sigma(y)}. \tag{15}$$

Using the consistency relation (11) just found, the action reads

$$S_B \sim \int dy e^{4\Lambda(y)+(1/4)\Lambda(y)+(\lambda/2)\sqrt{3M^3}\Lambda(y)} S_{(4)}, \tag{16}$$

where $S_{(4)}$ is the remaining part of the action. According to the solution $\Lambda(y) = 2a\,\mathrm{lnsechy}$ [cf. Eqs. (11)–(13)] the 5D factor is finite

$$\int dy e^{c\Lambda} = \int dy \cosh^{-2ac} y < \infty, \tag{17}$$

provided $c \equiv (17 + 2\lambda\sqrt{3M^3})/4 > 0$, namely $\lambda > -\frac{17}{2\sqrt{3M^3}} = \lambda_0$.

Studying the fluctuations of the metric about the above background configuration, it is possible to see that this model supports a massless zero mode of the gravitational field localized on the membrane even in the presence of the dilaton. In order to prove the stability of the background solution, we would have to show that there are no negative mass solutions to the equations of motion of a perturbation $h_{\mu\nu}$ of the metric. Actually, a gravitational Kaluza-Klein spectrum appears, starting from zero and presenting no gap. This can be easily seen after an appropriate change of variables and decomposition of the gravitational field, and a subsequent supersymmetric-type expression of the Schrödinger-type operator resulting from the equation of motion (see [3,11] for details). The issue of the coupling of these massive modes to the brane has been analyzed in detail in [12].

III. GAUGE-FIELD ACTION IN A WARPED SPACE WITH DILATON

Let us consider the following 5D action where a five-dimensional electromagnetic field A_N is coupled to the dilaton [13] in a warped space-time

$$S_g = \int dy d^4x \sqrt{-\det G_{AB}} e^{-(\lambda/2)\Pi}\left\{-\frac{1}{4}F_{MN}F^{MN}\right\}, \tag{18}$$

where $F_{MN} = \partial_{[M}A_{N]}$.

Assuming that the gauge-field energy density should not strongly modify the geometrical background, we can study the behavior of the propagating modes in the background of the topological configuration studied in the last section. In general, most of the attempts to stabilize 5D brane-worlds by means of a scalar field in the bulk do not take into account the backreaction of the scalar field on the background metric [3,11,12,14] and those in order to compute the scalar backreaction on the metric were unsuccessful except in a few special cases [9,15].

The factor $\exp(\Sigma - \lambda\Pi/2)$, present in the integrand, will lead to a change in the integration measure which is crucial to conserve the effect of the warping function on the 4D gauge field. As a consequence, zero modes (namely photons) are normalizable in the 4D effective theory. To

see it in detail, we need to solve the 5D equations of motion for A_M:

$$\frac{1}{\sqrt{-G}}\partial_M(G^{MR}G^{NP}F_{RP}\sqrt{-G}e^{-(\lambda/2)\Pi(y)}) = 0, \quad (19)$$

where $\mathrm{diag}\, G_{MN} = (e^{2\Lambda}\eta_{\mu\nu}, e^{2\Sigma})$. For this, we adopt the following gauge choice $A^5 = 0$, $\partial_\mu A^\mu = 0$ and separate the fifth from the ordinary coordinates as follows:

$$A^\mu(x, y) = a^\mu(x)u(y). \quad (20)$$

Now, from Eq. (19) we just get

$$\left[\Box + \frac{1}{uf}\partial_5(f\partial^5 u)\right]a^\mu = 0. \quad (21)$$

Note that the warped metric and the dilaton deform the solutions of this differential equation by means of the factor $f(y) \equiv e^{4\Lambda+\Sigma-\lambda\Pi/2}$ multiplying $u(y)$ and $u'(y)$. A full Kaluza-Klein spectrum results from the solution of the general case

$$\partial_5(f\partial^5 u) = -m^2 f u, \quad (22)$$

where m^2 is an arbitrary constant representing the 4D squared boson mass of the vector gauge field. It means that $a^\mu = a^\mu(0)e^{ipx}$ with $p^2 = -m^2$.

By expanding Eq. (21), we obtain the most general y-dependent equation of motion for the modified sine-Gordon potential (14) derived from action (18) in a form which exhibits its dependence on $a = \frac{1}{6}M^3b^2$ and c:

$$u''(y) + a(1-2c)\tanh y u'(y) + m^2\mathrm{sech}^a y u(y) = 0, \quad (23)$$

where $y \in (-\infty, \infty)$ as already stated. Looking back at the definition of the auxiliary constants, we get the explicit dependence of the solutions on the original parameters b, λ, and M.

Below, we will discuss the possible values of m^2 as resulting from an eigenvalue problem related to the equation of motion (23). Indeed, there exists a Schrödinger-like equation equivalent to Eq. (23) with a potential function which concentrates all the richness implicit in the complicated Eq. (23). Note that the particular solution $u(y) =$ constant represents the $m^2 = 0$ *photon* state of the 5D theory. Since this solution satisfies Eq. (23) for any value of a and c, any member of the family of problems has a guaranteed localized zero mode. See [5] for details.

Localization of gauge-field modes in the ordinary space can be established by verifying that the corresponding 5D action is finite. From Eq. (20), one has $F^{\mu\nu} = f^{\mu\nu}u(y)$, where $f^{\mu\nu} = G^{\mu\alpha}G^{\nu\beta}f_{\alpha\beta}$, so that for a gauge mode A_M^{sol} the relevant part of Eq. (18) reads

$$S_g[A_M^{\mathrm{sol}}] = \int dy u^2(y)e^{4\Lambda(y)+\Sigma(y)-\lambda\Pi(y)/2}\int d^4x\frac{1}{4}f_{\mu\nu}f^{\mu\nu}. \quad (24)$$

Using the field solutions found in Eq. (7) and the equations thereafter, the fifth dimension factor will remain finite for each mode $u(y)$ growing below e^{ac} at infinity. Thus, any finite solution is a physically acceptable Kaluza-Klein state (as we have seen above, to have a finite 5D Planck mass and background action S_B we already need $c > 0$, i.e. $\lambda > \lambda_0$).

It is known that by means of a transformation

$$u(y) = e^{-\alpha\Lambda/2}U(z), \qquad \frac{dz}{dy} = e^{-\beta\Lambda}, \quad (25)$$

we can turn Eq. (23) into a Schrödinger-like equation in the variable z (see e.g. [2,3]). In general, the existence of an analog Schrödinger equation is useful to give us a feeling of the physical profile of the solutions of the original problem, as e.g. parity and eigenvalues. With $\alpha = c - 1/4$ and $\beta = -1/4$, we can eliminate the first derivative term in U and have a pure mass term as usual. The resulting differential equation reads precisely

$$\left[-\frac{d^2}{dz^2} + \mathfrak{V}_a(z)\right]U(z) = m^2U(z),$$

where $\mathfrak{V}_a(z) = e^{-\Lambda/2}(\frac{\alpha}{2}\Lambda'' - \gamma\Lambda'^2)$ and $\gamma = \frac{1}{4}\alpha(\frac{1}{2} - \alpha)$. In a few cases the last expression can be inverted after exact integration in order that an analytical expression for the analog nonrelativistic potential comes about. In Ref. [5] we have solved the $a = 2$ case and found

$$\mathfrak{V}_2(z) = -2\alpha[1 - (2\alpha - 1)\tan^2 z].$$

In this paper, for $a = 4$ we find

$$\mathfrak{V}_4(z) = \frac{(\gamma - \omega z^2)}{(1 - z^2)^2},$$

where γ and ω are constants and we shall analyze it in what follows.

IV. THE QUANTUM ANALOG

In the present case we can turn Eq. (23) into a Sturm-Liouville problem by means of

$$z = \tanh y, \quad (26)$$

$$u(y) = (\cosh y)^{4c-1}U(z) \quad (27)$$

[see Eq. (25)]. Now, we have a related Schrödinger equation defined in the z variable

$$\left[-\frac{d^2}{dz^2} + \mathfrak{V}_4(z)\right]U(z) = m^2U(z), \quad (28)$$

with

$$\mathfrak{V}_4(z) = \frac{1 - 4c}{(1 - z^2)^2}[1 + 2(1 - 2c)z^2]. \quad (29)$$

We can see that the potential function diverges at $z = \pm 1$ and so the boundary conditions of this analog problem are $\{U(z = \pm 1) = 0, U'(z = \pm 1)\text{finite}\}$ which must be in order to match finite $u(y)$ solutions to Eq. (23) at $y \to \pm\infty$.

After solving the quantum analog, we have to transform back variables and functions to check the finiteness and continuity of the original solution $u(y)$ in order to be physically acceptable.

We now better introduce the variable θ by means of

$$z = \cos\theta \tag{30}$$

which results in equation

$$U''(\theta) - \cot(\theta)U'(\theta) - \frac{1-4c}{\sin^2\theta}[1 + 2(1-2c)\cos^2\theta]U(\theta) = -m^2\sin^2\theta U(\theta) \tag{31}$$

for the analog wave function $U(\theta)$ with $U(\theta = \pi, 0) = 0$.

According to the arguments of localization seen in the previous section, physically acceptable solutions require $c > 0$ so we shall be restricted to that region.

A. The $c = 1/4$ case

Equation (31) gets strongly simplified for the value $c = 1/4$. In this case we obtain

$$\frac{1}{\sin\theta}\frac{d}{d\theta}\left(\frac{1}{\sin\theta}U'(\theta)\right) + m^2\sin^2\theta U(\theta) = 0 \tag{32}$$

with solutions

$$U^{(1)}(\theta) = U_0\sin(m\cos(\theta)) \tag{33}$$

$$U^{(2)}(\theta) = U_0\cos(m\cos(\theta)), \tag{34}$$

which in terms of the original variable and function read

$$u^{(1)}(y) = u_0\sin(m\tanh y) \tag{35}$$

$$u^{(2)}(y) = u_0\cos(m\tanh y) \tag{36}$$

(see Figs. 2 and 3). The zero mode, $m = 0$, is then related to $u(y) = u_0$ as already mentioned.

Since $\mathfrak{V}(z)$ is an even function (in this case trivial), solutions must have definite parity. Besides, the potential divergence at $z = \pm 1$ implies that the corresponding solutions are expected to be zero there. Thus, antisymmetric solutions correspond to the eigenvalues of the Schrödinger equation (28) $m = n\pi$ while symmetric solutions correspond to $m = (2n+1)\pi/2$, with $n \in N$ [or simply $m = (n+1)\pi/2$ with n even for symmetric solutions and odd for the antisymmetric ones].

B. Other analytical solutions

If we perform the transformation

$$U(\theta) = \sin^\kappa\theta\,\mathcal{M}(\theta), \tag{37}$$

in place of Eq. (31) we get the following problem for $\mathcal{M}(\theta)$:

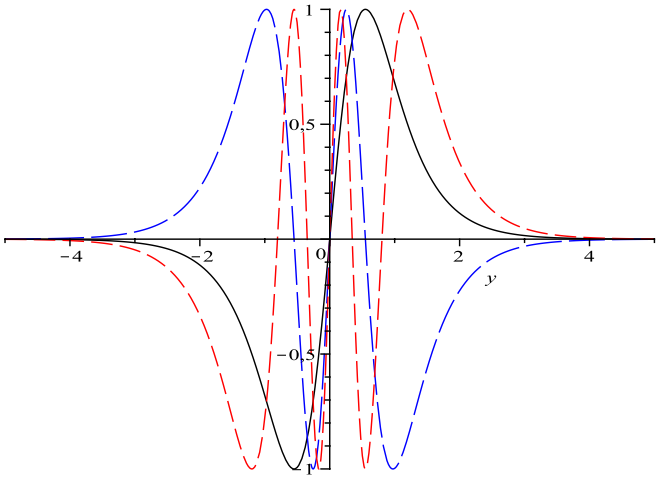

FIG. 2 (color online). Plot of $\sin(m\tanh(y))$, for $c = 1/4$, $m = \pi$ (black line), $m = 2\pi$ (long-dashed blue line), and $m = 3\pi$ (dashed red line).

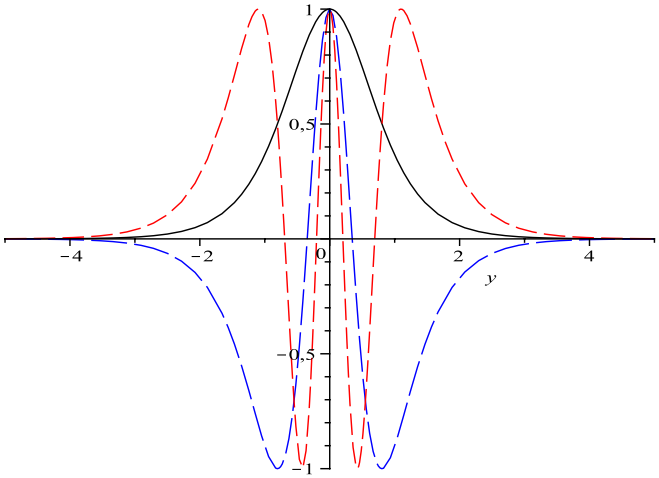

FIG. 3 (color online). Plot of $\cos(m\tanh(y))$, for $c = 1/4$, $m = \pi/2$ (black line), $m = 3\pi/2$ (long-dashed blue line), and $m = 5\pi/2$ (dashed red line).

$$\mathcal{M}''(\theta) + (2\kappa - 1)\cot(\theta)\mathcal{M}'(\theta) + \left[\kappa(\kappa-2)\cot^2(\theta) - \kappa + \frac{1-4c}{\sin^2\theta}[1 + 2(1-2c)\cos^2\theta]\right]\mathcal{M}(\theta) = -m^2\sin^2\theta\,\mathcal{M}(\theta). \tag{38}$$

Now, we can choose a convenient power for the last transformation, $\kappa = 1/2$, in order to turn this into

$$\mathcal{M}''(\theta) - 4\left[\cot^2(\theta)\left(4c^2 - 4c + \frac{15}{16}\right) + \frac{3}{8} - c\right]\mathcal{M}(\theta) = -m^2\sin^2\theta\,\mathcal{M}(\theta) \tag{39}$$

which, for $4c^2 - 4c + \frac{15}{16} = 0$, is known as the Mathieu differential equation

$$M''(\theta) + (4c - 3/2 + m^2\sin^2\theta)M(\theta) = 0, \quad (40)$$

with $c = 3/8$ or $c = 5/8$.

C. The case $c = 5/8$

In this case, Eq. (40) results in

$$M''(\theta) + \left(1 + \frac{m^2}{2} - \frac{m^2}{2}\cos(2\theta)\right)M(\theta) = 0 \quad (41)$$

whose analytic solutions are the general Mathieu functions

$$M^{(1)}(\theta) = Mc\left(1 + \frac{m^2}{2}, \frac{m^2}{4}, \theta\right) \quad (42)$$

$$M^{(2)}(\theta) = Ms\left(1 + \frac{m^2}{2}, \frac{m^2}{4}, \theta\right), \quad (43)$$

which, in terms of the z variable, result in the analog wave functions $U(z)$:

$$U^{(1)}(z) = (1 - z^2)^{1/4}Mc\left(1 + \frac{m^2}{2}, \frac{m^2}{4}, \arccos(z)\right) \quad (44)$$

$$U^{(2)}(z) = (1 - z^2)^{1/4}Ms\left(1 + \frac{m^2}{2}, \frac{m^2}{4}, \arccos(z)\right) \quad (45)$$

(see [16] for details about Mathieu functions).

As mentioned above, the boundary conditions of the present problem are $\{U(z = \pm 1) = 0, U'(z = \pm 1)\text{finite}\}$, related to finite $u(y)$ solutions to the original equation, recalling that $y \in (-\infty, \infty)$. The first set of solutions, $U^{(1)}(z)$, is not physically interesting because the derivatives of these functions are divergent at the boundary. The reason is that $Mc(\arccos(z))$ cannot be zero at $z = 1$ for any value of m. The second set, on the other hand, has physically acceptable solutions for a discrete set of values of m, the (twenty) first of which we show in Table I. These solutions are symmetric or antisymmetric, as expected (see Fig. 4). Note the presence of a zero mode.

TABLE I. List of the first 21 values of m_s (symmetric solutions) and m_a (antisymmetric ones) for $c = 5/8$.

m_s	m_a
0.000 000 0	– –
4.064 986 0	2.380 795 9
7.296 211 5	5.691 401 9
10.478 088 0	8.890 261 3
13.643 145 8	12.061 959 6
16.800 275 6	15.222 418 5
19.952 989 30	18.377 053 8
23.102 972 0	21.528 253 1
26.251 140 9	24.677 243 35
29.398 071 6	27.824 723 8
32.544 043 9	30.971 123 52
...	...

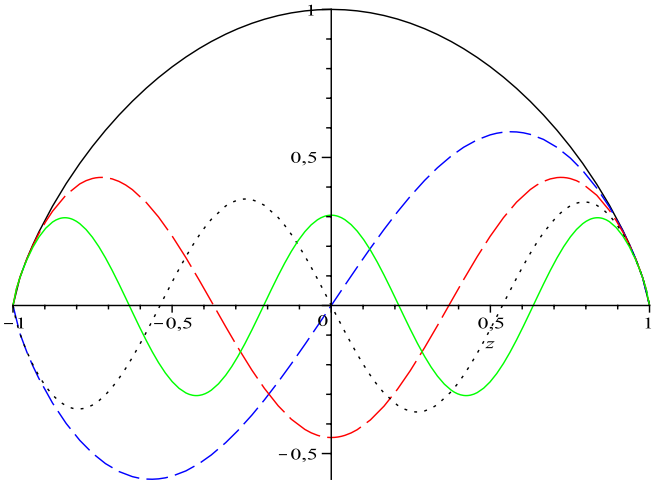

FIG. 4 (color online). Symmetric and antisymmetric eigenfunctions U in z space for $c = 5/8$; $m = 0$ (black line, symmetric), $m = 2.380\,795\,874$ (dashed blue line, antisymmetric), $m = 4.064\,9860$ (long-dashed red line, symmetric), $m = 5.691\,4019$ (dotted black line, antisymmetric), and $m = 7.296\,2115$ (solid green line, symmetric).

In terms of y, we have

$$u^{(1)}(y) = \cosh y Mc\left(1 + \frac{m^2}{2}, \frac{m^2}{4}, \arccos(\tanh y)\right) \quad (46)$$

$$u^{(2)}(y) = \cosh y Ms\left(1 + \frac{m^2}{2}, \frac{m^2}{4}, \arccos(\tanh y)\right), \quad (47)$$

where the set $u^{(1)}(y)$ diverges when $y \to \pm\infty$, as due from the comments above, so we just keep the solutions $u^{(2)}(y)$ (see Figs. 5 and 6).

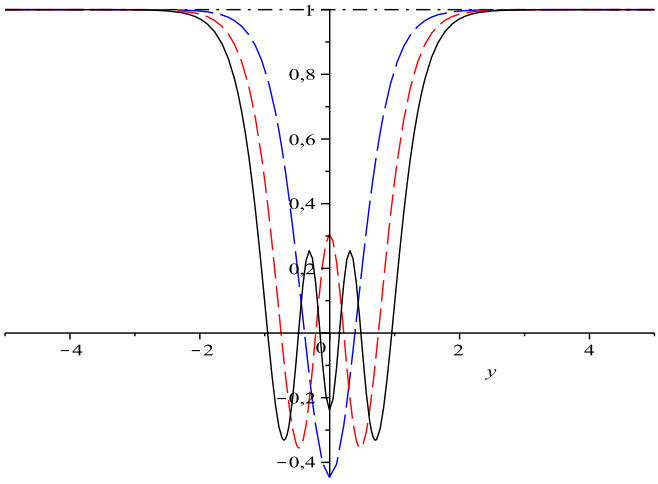

FIG. 5 (color online). Symmetric solutions $u^{(2)}(y)$ [Eq. (47)] for $c = 5/8$; $m = 0$ (dash-dotted black line), $m = 4.064\,986\,0$ (long-dashed blue line), $m = 7.296\,211\,5$ (dashed red line), and $m = 10.478\,088\,0$ (solid black line).

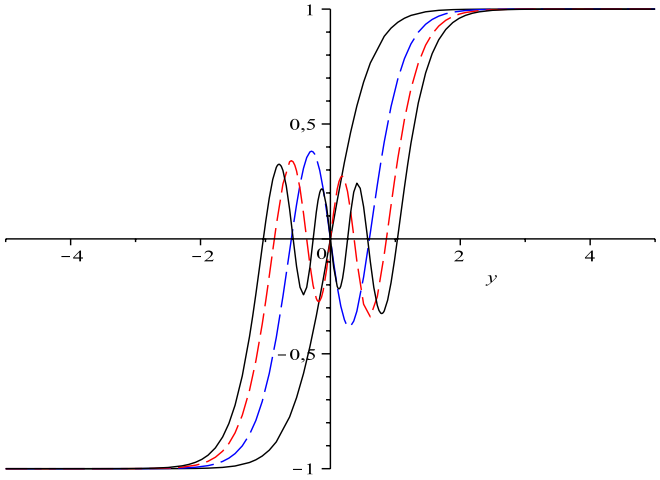

FIG. 6 (color online). Antisymmetric solutions $u^{(2)}(y)$ for $c = 5/8$; $m = 2.380\,795\,9$ (solid black line), $m = 5.691\,401\,9$ (long-dashed blue line), $m = 8.890\,261\,3$ (dashed red line), and $m = 12.061\,959\,6$ (solid black line).

D. The case $c = 3/8$

Now, Eq. (40) reads

$$M''(\theta) + \left(\frac{m^2}{2} - \frac{m^2}{2}\cos(2\theta)\right)M(\theta) = 0 \tag{48}$$

with solutions given by

$$M^{(1)}(\theta) = Mc\left(\frac{m^2}{2}, \frac{m^2}{4}, \theta\right) \tag{49}$$

$$M^{(2)}(\theta) = Ms\left(\frac{m^2}{2}, \frac{m^2}{4}, \theta\right), \tag{50}$$

corresponding to

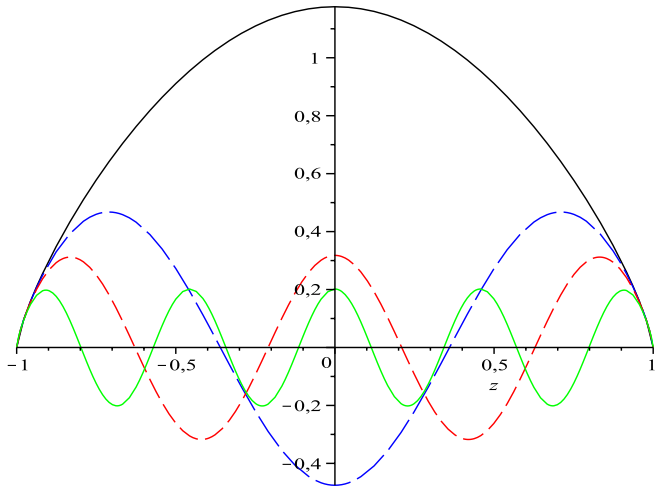

FIG. 7 (color online). Symmetric solutions $U^{(2)}(z)$ for $c = 3/8$; $m = 1.147\,180\,42$ (solid black line), $m = 4.302\,069\,64$ (long-dashed blue line), $m = 7.448\,792\,88$ (dashed red line), and $m = 13.736\,298\,72$ (solid green line).

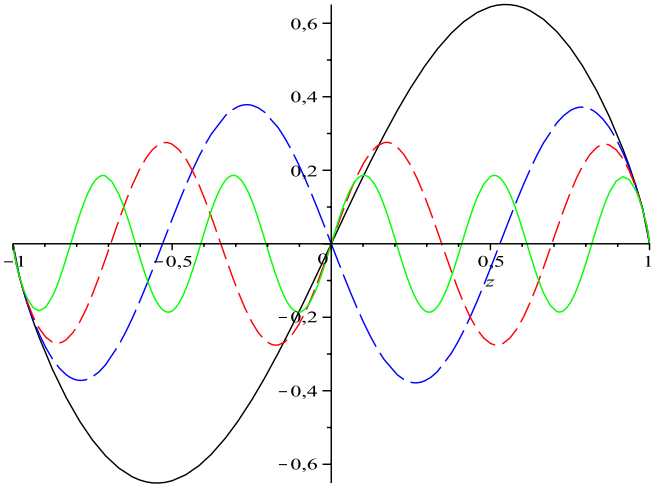

FIG. 8 (color online). Antisymmetric solutions $U^{(2)}(z)$ for $c = 3/8$; $m = 2.726\,324\,77$ (solid black line), $m = 5.875\,920\,07$ (long-dashed blue line), $m = 9.021\,100\,25$ (dashed red line), and $m = 15.307\,712\,12$ (solid green line).

$$U^{(1)}(z) = (1 - z^2)^{1/4} Mc\left(\frac{m^2}{2}, \frac{m^2}{4}, \arccos(z)\right) \tag{51}$$

$$U^{(2)}(z) = (1 - z^2)^{1/4} Ms\left(\frac{m^2}{2}, \frac{m^2}{4}, \arccos(z)\right) \tag{52}$$

in the z space with the boundary conditions already seen.

As we discussed in the previous ($c = 5/8$) case, only the second set of solutions is physically relevant and just for a discrete (infinite) sequence of m eigenvalues. For such values solutions have definite parity according to $\mathfrak{V}(z)$, Eq. (29) (see Figs. 7 and 8).

Note that the solutions to the Schrödinger equation [the analytical expressions (51) and (52)] are not compatible with a zero mode for the z-boundary conditions given above. Actually, as a general result, for any value excluded from the sequence starting in Table II, $U^{(1)}(z)$—Eq. (51)—has divergent derivatives at $z = \pm 1$ and

TABLE II. List of the first 20 values of m_s and m_a for $c = 3/8$.

m_s	m_a
— —	— —
1.147 180 42	2.726 324 77
4.302 069 64	5.875 920 07
7.448 792 88	9.021 100 25
10.593 050 44	12.164 759 84
13.736 298 72	15.307 712 12
16.879 030 28	18.450 274 34
20.021 459 51	21.592 597 04
23.163 695 47	24.652 708 00
26.305 799 84	27.876 815 05
29.447 810 28	31.018 788 23
...	...

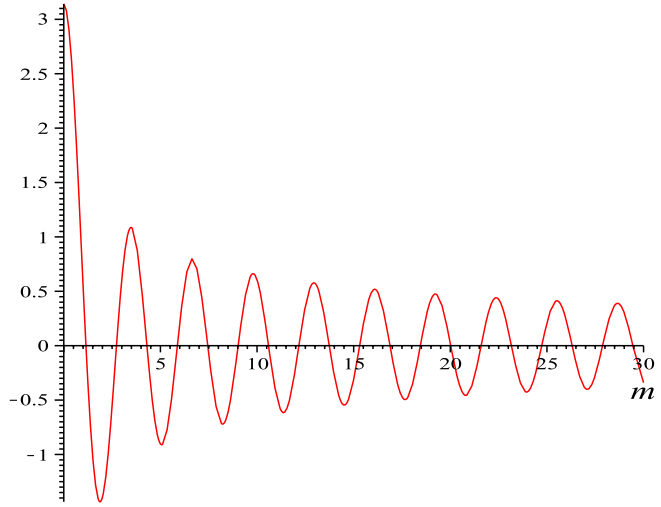

FIG. 9 (color online). Mathieu function at the boundary ($\theta = \pi$) as a function of the mass for $c = 3/8$, $Ms(\frac{m^2}{2}, \frac{m^2}{4}, \theta = \pi)$. At the other boundary, $Ms(\frac{m^2}{2}, \frac{m^2}{4}, \theta = 0) = 0$.

$U^{(2)}(z)$—Eq. (52)—is not even symmetric. For this reason the zero-mass solutions of Eq. (48), $M(\theta, m = 0) \in \{\text{cons}, \theta\}$, do not correspond to valid solutions of the Schrödinger problem. In Fig. 9 we can see all the first mass values of the sequence which nullify the Mathieu functions Ms at the boundary. These values, also listed in Table II, guarantee finite derivatives of $U^{(2)}(z)$. The absence of the zero mode in this list indicates a limitation of the Schrödinger analogue approach. We will come again to this point in the next section. In terms of y we have

$$u^{(1)}(y) = Mc\left(\frac{m^2}{2}, \frac{m^2}{4}, \arccos(\tanh y)\right) \tag{53}$$

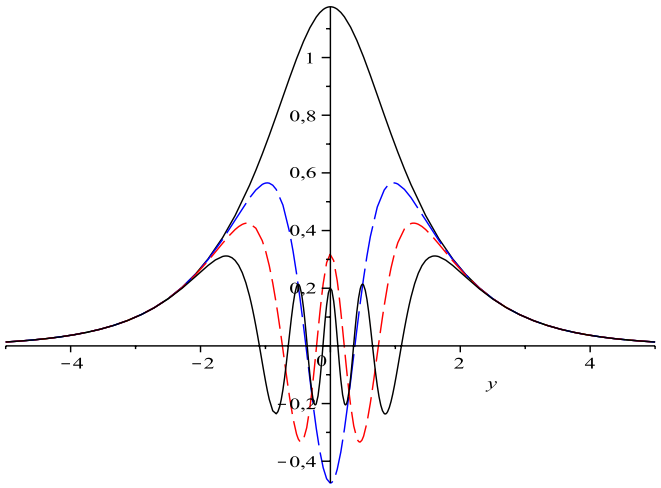

FIG. 10 (color online). Symmetric solutions $u^{(2)}(y)$, Eq. (54), for $c = 3/8$; $m = 1.147\,180\,42$ (solid black line), $m = 4.302\,069\,64$ (long-dashed blue line), $m = 7.448\,792\,88$ (dashed red line), and $m = 13.736\,298\,72$ (solid black line).

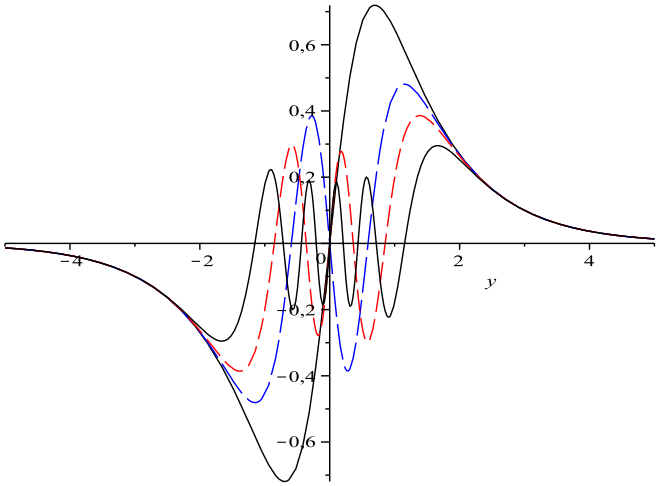

FIG. 11 (color online). Antisymmetric solutions $u^{(2)}(y)$, Eq. (54), for $c = 3/8$; $m = 2.726\,324\,77$ (solid black line), $m = 5.875\,920\,07$ (long-dashed blue line), $m = 9.021\,100\,25$ (dashed red line), and $m = 15.307\,712\,12$ (solid black line).

$$u^{(2)}(y) = Ms\left(\frac{m^2}{2}, \frac{m^2}{4}, \arccos(\tanh y)\right), \tag{54}$$

of which $u^{(2)}$ represents the only nondivergent set of solutions, as we illustrate in Figs. 10 and 11 for the first quantum values of m.

V. THE CONFLUENT HEUN EQUATION

We now investigate our original problem by relaxing the quantum analog condition. In order to obtain the general solution of Eq. (23) we perform the following change of variable:

$$x = \tanh y. \tag{55}$$

It maps the y space to $x \in (-1, 1)$ and we will eventually transform it back in order to come into the original space and variables. Note that Eq. (23) is symmetric under a parity transformation and thus the differential equation admits even as well as odd parity solutions, as it should. Now, Eq. (23) becomes

$$u''(x) + (2 - \tilde{c})\frac{x}{x^2 - 1}u'(x) + m^2(1 - x^2)^{(a/2)-2}u(x) = 0, \tag{56}$$

which is an homogeneous second-order linear differential equation with polynomial coefficients provided a is even. Here $\tilde{c} = a(1 - 2c)$ so that $\tilde{c} = (-\infty, a)$. Now, Eq. (56) looks more familiar if we change x^2 into z:

$$u''(z)+\left(\frac{1/2}{z}+\frac{1-\tilde{c}/2}{z-1}\right)u'(z)+\frac{m^2}{4}\frac{u(z)}{z}=0, \quad (57)$$

for the case under study. Formally, this equation has two regular singular (Fuchsian) points at $z=0,1$, and an irregular one at $z=\infty$. This is known as a confluent Heun equation [17–19].

We can compare Eq. (57) with the canonical nonsymmetrical general form of the confluent Heun equation as given in [18–20],

$$Hc''(z)+\left(\alpha+\frac{\beta+1}{z}+\frac{\gamma+1}{z-1}\right)Hc'(z)+\left[\frac{[\delta+\frac{\alpha}{2}(\beta+\gamma+2)]z+\eta+\frac{\beta}{2}+\frac{1}{2}(\gamma-\alpha)(\beta+1)}{z(z-1)}\right]Hc(z)=0, \quad (58)$$

whose solutions around $z=0$ are denoted by

$$H^{(1)}=Hc(\alpha,\beta,\gamma,\delta,\eta;z) \quad (59)$$

$$H^{(2)}=z^{-\beta}Hc(\alpha,-\beta,\gamma,\delta,\eta;z). \quad (60)$$

In general, there are two linearly independent local series solutions around each singular point. In the region of interest, $z<1$, we look for a regular local solution around $z=0$ which is defined by the Heun series as

$$Hc(z)=\sum_{n=0}^{\infty}d_n z^n. \quad (61)$$

Here the constants d_n (with $d_{-1}=0$ and $d_0=1$) are determined by the three-term recurrence relation [21]

$$A_n d_n=B_n d_{n-1}+C_n d_{n-2}, \quad (62)$$

where

$$A_n=1+\frac{\beta}{n}\to 1-\frac{1}{2n} \quad (63)$$

$$B_n=1+\frac{-\alpha+\beta+\gamma-1}{n}+\frac{\eta+(\alpha-\beta-\gamma)/2-\alpha\beta/2+\beta\gamma/2}{n^2}\to 1+\frac{-\tilde{c}/2-3/2}{n}+\frac{\tilde{c}/2+1/2-m^2/4}{n^2} \quad (64)$$

$$C_n=\frac{1}{n^2}\left(\delta+\frac{\alpha(\beta+\gamma)}{2}+\alpha(n-1)\right)\to\frac{m^2}{4n^2}. \quad (65)$$

By comparing Eqs. (57) and (58), it is easy to identify $\alpha=0$, $\beta=-1/2$, $\gamma=-\tilde{c}/2$, $\delta=m^2/4$, and $\eta=\tilde{c}/8+1/4-m^2/4$. Then the solutions of Eq. (23) are given by

$$u^{(1)}(y)=Hc\left(0,-\frac{1}{2},-\frac{\tilde{c}}{2},\frac{m^2}{4},\frac{1}{4}+\frac{\tilde{c}}{8}-\frac{m^2}{4};\tanh^2 y\right) \quad (66)$$

$$u^{(2)}(y)=\tanh y Hc\left(0,\frac{1}{2},-\frac{\tilde{c}}{2},\frac{m^2}{4},\frac{1}{4}+\frac{\tilde{c}}{8}-\frac{m^2}{4};\tanh^2 y\right) \quad (67)$$

for arbitrary values of $\tilde{c}$ (or c), namely, of the dilaton coupling constant. The conditions these Heun $u(y)$ solutions must obey to be acceptable are the original ones, i.e. finiteness and continuity in the whole space.

A noteworthy point in the present approach is that now, depending on $\tilde{c}$, the mass values m^2 can be quantized, as we saw in Sec. IV, or not, as we will explain in what follows.

After a lengthy numerical exam, we found clear evidence that for $\tilde{c}\leq 0$ (namely $\lambda\geq\lambda_1\equiv 15/17\lambda_0$) all the mass spectra are discrete. For $\tilde{c}\in(0,4)$, $\lambda_0<\lambda<\lambda_1$, on the other hand, the corresponding spectra start with a zero mode and grow continuously. This sharp contrast may be traced back to Eq. (23) where the second term of the differential equation flips precisely with the sign of $\tilde{c}$. Note that for any well-behaved solution $u(y)$, the third term of Eq. (23) can be disregarded at infinity. The remainder differential equation can be easily solved showing that, for $\tilde{c}>0$, solutions are always convergent to zero and for $\tilde{c}\leq 0$ they diverge at the boundary. Guided by this result, we performed a numerical survey in each region arriving at the conclusion above: for $\tilde{c}>0$ there exist physical solutions for arbitrary m while, otherwise, only a discrete sequence of masses allow for finite solutions at the border.

It should be mentioned that for small values of $\tilde{c}$ the solutions stabilize quickly. On the contrary, for $\tilde{c}\lesssim -10$ the numerical calculation is more difficult and more digits are needed in the mass precision to stabilize solutions at large values of y. For example, for $\tilde{c}=-30$, which corresponds to $\lambda=0$, more than 30 significant digits were necessary in the mass spectrum to find the solutions as shown in Figs. 12 and 13. In Table III we listed the first values of the mass up to the eighth decimal place.

As awaited, for the cases studied in the previous section we find again the same results. Note however that the zero mode in the $\tilde{c}=1(c=3/8)$ case now appears explicitly. This was expected since there exists an analytical $m=0$ solution to Eq. (23), namely $u_0(y)=e_1\arctan(e^y)+e_2$, which must be present in a full approach. Furthermore, for $\tilde{c}=1$ the Heun solution indicates that Table II would not only start from zero but would also be continuously filled in as mentioned above. In Figs. 14 and 15 we can see finite analytic Heun solutions, given by Eqs. (66) and (67), for some arbitrary values of m besides the quantum-mechanical analog ones. Another way to see it is by means of Figs. 16 and 17 where m has been fixed arbitrarily to one of the eigenvalues of $\tilde{c}=1$ and $\tilde{c}$ is then varied. In the

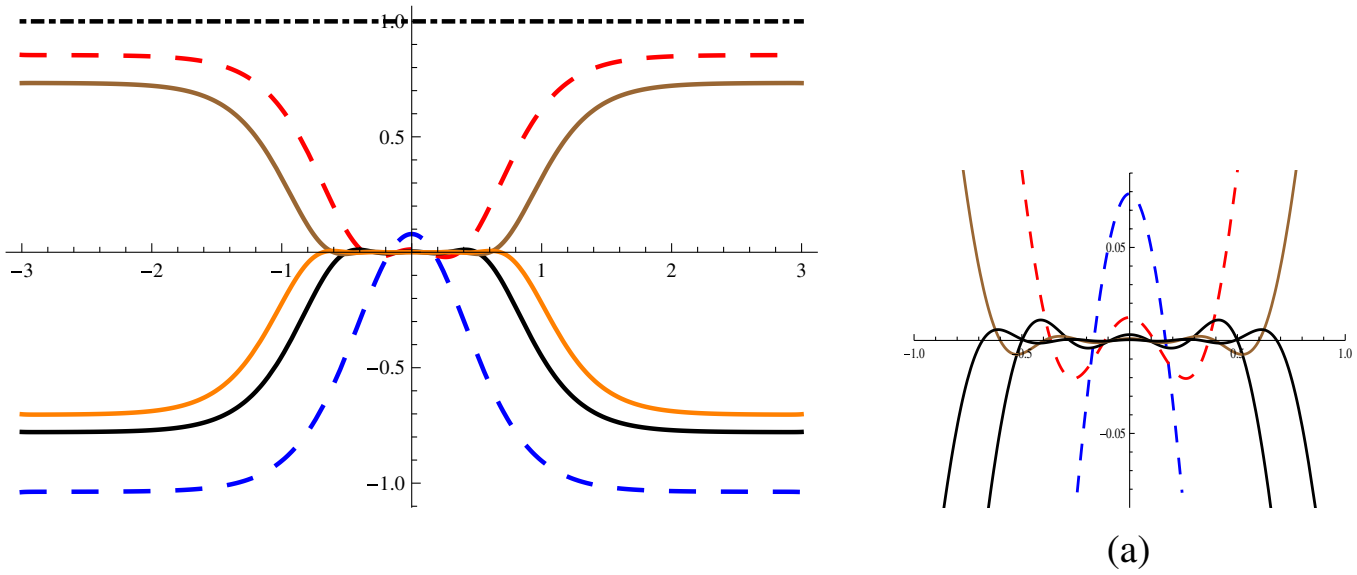

FIG. 12 (color online). Symmetric solutions of the Heun equation ($\tilde{c} = -30$) for $m = 0$ (black dash dotted), $m = 8.693\,553\,30$ (blue dashed), $m = 13.168\,601\,26$ (red dashed), $m = 17.106\,433\,40$ (black solid), $m = 20.803\,071\,54$ (brown solid), $m = 24.362\,698\,18$ (orange solid). Curves required masses with 30 significant digits of which only the first are shown. (a) Solutions Eq. (66) near the origin.

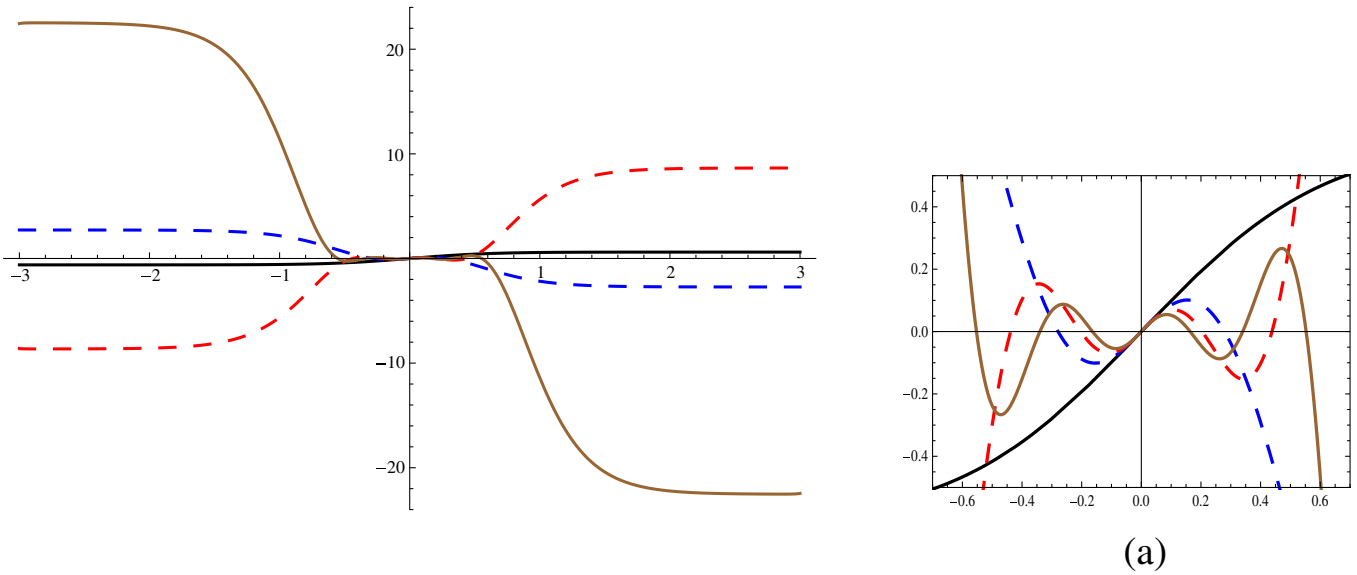

FIG. 13 (color online). Antisymmetric solutions of the Heun equation ($\tilde{c} = -30$) for $m = 5.909\,530\,31$ (black solid), $m = 11.035\,472\,47$ (blue dashed), $m = 15.178\,367\,81$ (red dashed), $m = 18.97642242$ (brown solid). (a) Solutions Eq. (67) near the origin.

$\tilde{c} = -1 (c = 5/8)$ case, the spectrum still obeys quantized values as given in Table I.

Thus, although Mathieu functions have been sufficient to characterize a part of the spectrum of the Schrödinger analog of our problem, we actually need to consider confluent Heun functions to cover all the cases. In other words, even when we achieved fully analytical solutions of the quantum analog differential equation, the spectra appeared just discrete not revealing that some of them could be eventually continua.

The set of confluent Heun functions therefore provides all the possible physical solutions of the actual problem in the 5D space. This was not apparent from the Hamiltonian point of view which assumes the Sturm-Liouville operator $\mathcal{H} = [-\frac{d^2}{dz^2} + \mathfrak{V}(z)]$ to represent the physical situation.

TABLE III. List of first values of m_s and m_a for $\tilde{c} = -30$.

m_s	m_a
0	$--$
8.693 553 30	5.909 530 31
13.168 601 26	11.035 472 47
17.106 433 40	15.178 367 81
20.803 071 54	18.976 422 42
24.362 698 18	22.596 204 20
...	...

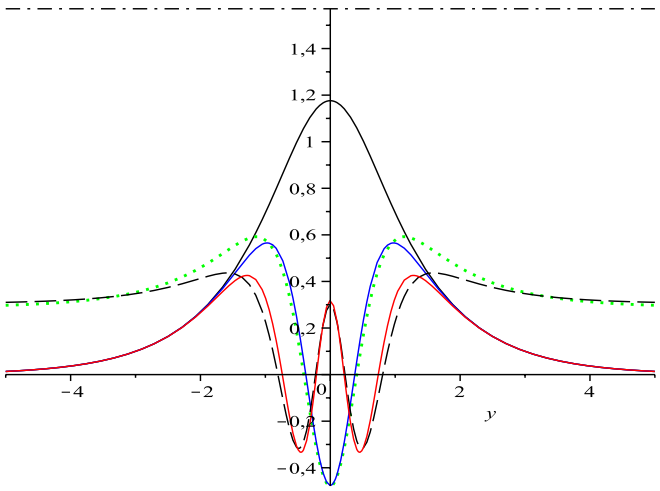

FIG. 14 (color online). Symmetric solutions [Eq. (66)] for $\tilde{c} = 1$; $m = 0$ (dash-dotted black line), $m = 1.147\,180\,42$ (solid black line), $m = 4$ (dotted green line), $m = 4.302\,069\,64$ (solid blue line), $m = 7$ (dashed black line), and $m = 7.448\,792\,88$ (solid red line).

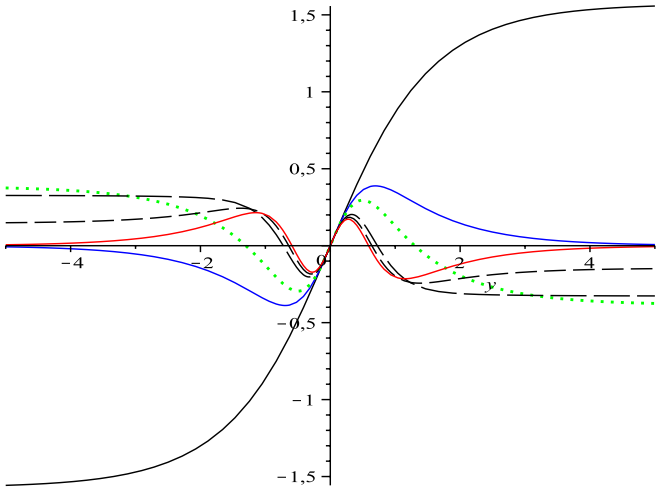

FIG. 15 (color online). Antisymmetric solutions [Eq. (67)] for $\tilde{c} = 1$; $m = 0$ (solid black line), $m = 2.726\,324\,772$ (solid blue line), $m = 3.5$ (dotted green line), $m = 5$ (long-dashed black line), $m = 5.5$ (dashed black line), and $m = 5.875\,920\,066$ (solid red line).

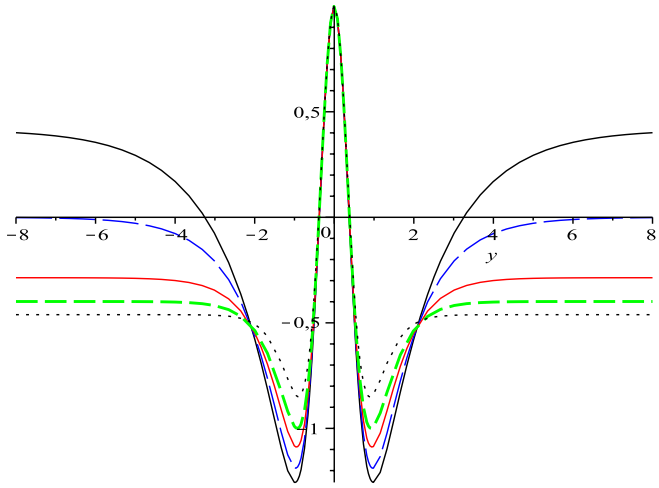

FIG. 16 (color online). Symmetric Heun solutions, Eq. (66), for $m = 4.302\,069\,64$ and several values of $\tilde{c}$: $\tilde{c} = 0.7$ (solid black line), $\tilde{c} = 1$ (long-dashed blue line), $\tilde{c} = 1.5$ (solid red line), $\tilde{c} = 2$ (dashed green line), and $\tilde{c} = 3$ (dotted black line).

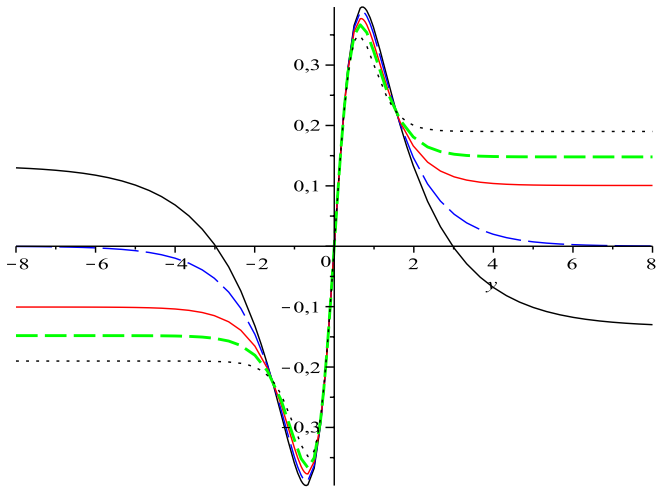

FIG. 17 (color online). Antisymmetric Heun solutions, Eq. (67), for $m = 2.726\,324\,77$ and several values of $\tilde{c}$: $\tilde{c} = 0.7$ (solid black line), $\tilde{c} = 1$ (long-dashed blue line), $\tilde{c} = 1.5$ (solid red line), $\tilde{c} = 2$ (dashed green line), and $\tilde{c} = 3$ (dotted black line).

VI. FINAL REMARKS AND CONCLUSION

In order to physically assess massive modes, one can evaluate the variation of the effective gauge coupling as a function of the Kaluza-Klein masses. Actually, KK contributions cannot be significant as compared with the Coulomb potential because the coupling of massive modes to (fermion) matter on the brane develops a Yukawa-type potential in the nonrelativistic limit. To show that this is a decreasing function of m, we should evaluate the

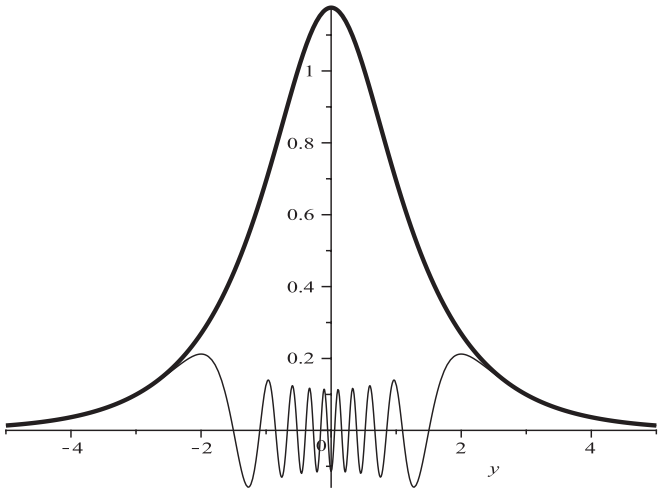

FIG. 18. First and tenth even KK eigenmodes exhibit their relative weights.

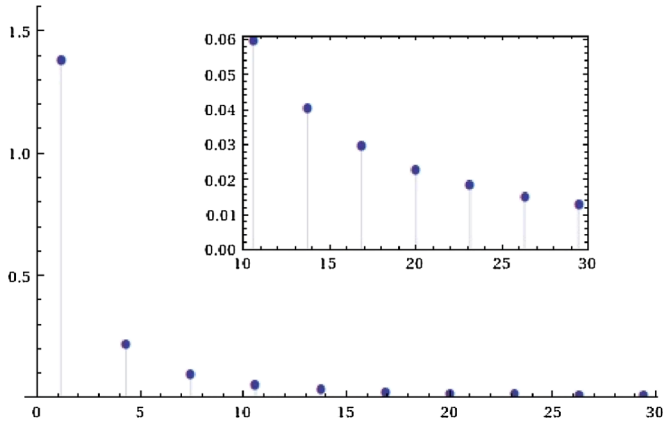

FIG. 19 (color online). Sequence of the first KK values of $u^2_{\text{even}}(0)$ for $c = 3/8$ displaying the relative weights of the KK modes on the brane.

coefficients that multiply the relevant sector of the four-dimensional action:

$$\sim \int dy e^{\Sigma - \lambda\Pi}\left(u^2_{m=0}(y) + \sum_n u^2_{m_n}(y)\right)\int d^4x f_{\mu\nu}f^{\mu\nu}. \quad (68)$$

However, in order to simplify this computation we can assume that the coupling with the brane takes place exactly on the 4D ordinary space-time, namely, at $y = 0$. It is precisely at this value of y where the relevant physical effects should be much stronger. For simplicity let us consider the series of the quantum analog eigenvalues which serves as a discrete representative of the continuum. Thus, the effective 4D electrostatic potential would read

$$V(r) \sim q_1 q_2\left(\frac{c_0^2}{r} + \sum_n \frac{e^{-m_n r}}{r} u^2_{m_n}(0)\right), \quad (69)$$

where q_1, q_2 are two test charges separated a distance r in ordinary 3D space and the Kaluza-Klein masses m are numbered with n in ascending order. See Fig. 14 where the first $u^{(1)}_{\text{even}}(y)$ modes are fully displayed, and Fig. 18 where the first and the tenth modes are compared. See Fig. 19 to appreciate the first ten values at the origin. This, together with the negative exponential factor, essentially decouples the massive modes from the physics on the domain wall. Far from the membrane, all massive modes become constants like the zero mode is, and as a consequence the 5D phenomenology results completely modified from ordinary 4D electromagnetism. See e.g. Refs. [2,12] for the study of this issue in the case of gravity.

In this paper we have studied bulk and four-dimensional gauge propagation modes in a warped extra-dimensional space with a dilaton field. We have set up a sine-Gordon thick membrane which bounces at the extra-coordinate origin. A five-dimensional metric was dynamically generated consistently with the soliton brane and the dilaton background. In such a framework we studied the solutions of a five-dimensional gauge field.

First, we have found the exact quantum-mechanical analog of our original five-dimensional stringy problem. We have shown that the corresponding Schrödinger potential function is a quotient of simple second- and fourth-order polynomials that we could solve analytically. We next obtained the exact quantum-mechanical analog eigenspectrum and used it as a guide to analyze eventually the general solution. A localized zero mode corresponding to the ordinary photon was guaranteed for a dilaton coupling constant above λ_0. In general, we have found that the gauge-field dynamics are analytically given by confluent Heun functions which we have displayed for several representative cases. Furthermore, in contrast to the quantum analog results, in the general approach the mass of the gauge-field modes can be arbitrary for $\lambda \in (\lambda_0, \lambda_1)$. In any case, we have shown that the Kaluza-Klein gauge spectrum is strongly attenuated on the brane as compared to the zero mode of the theory. On the other hand, we observed that in the bulk, far from the brane, the amplitude of an infinite tower of massive modes gets progressively relevant. Interestingly, the quantum-mechanical discrete mass eigenfunctions are completely decoupled in that region.

[1] J. Polchinski, *String Theory* (Cambridge University Press, Cambridge, England, 1998), Vols. 1&2.

[2] L. Randall and R. Sundrum, Phys. Rev. Lett. **83**, 4690 (1999); **83**, 3370 (1999).

[3] A. Kehagias and K. Tamvakis, Phys. Lett. B **504**, 38 (2001).

[4] D. Youm, Nucl. Phys. **B589**, 315 (2000); Phys. Rev. D **64**, 127501 (2001).

[5] H. R. Christiansen, M. S. Cunha, and M. K. Tahim, Phys. Rev. D **82**, 085023 (2010).

[6] Y.-X. Liu *et al.*, J. High Energy Phys. 06 (2011) 135; Chun-E Fu, Yu-Xiao Liu, and Heng Guo, Phys. Rev. D **84**, 044036 (2011); Y.-X. Liu *et al.*, arXiv:1102.4500; R. R. Landim *et al.*, J. High Energy Phys. 08 (2011) 071.

[7] G. Dvali and M. Shifman, Phys. Lett. B **396**, 64 (1997); **407**, 452(E) (1997); G. Dvali, G. Gabadadze, and M. Shifman, Phys. Lett. B **497**, 271 (2001).

[8] M. Cvetic, S. Griffies, and S. Rey, Nucl. Phys. **B381**, 301 (1992).

[9] O. DeWolfe, D. Z. Freedman, S. S. Gubser, and A. Karsch, Phys. Rev. D **62**, 046008 (2000).

[10] K. Skenderis and P. K. Townsend, Phys. Lett. B **468**, 46 (1999).

[11] M. Gremm, Phys. Lett. B **478**, 434 (2000).

[12] C. Csaki, J. Erlich, T. J. Hollowood, and Y. Shirman, Nucl. Phys. **B581**, 309 (2000); C. Csaki, J. Erlich, and T. J. Hollowood, Phys. Rev. Lett. **84**, 5932 (2000).

[13] P. Mayr and S. Stieberger, Nucl. Phys. **B412**, 502 (1994).

[14] W. D. Goldberger and M. B. Wise, Phys. Rev. Lett. **83**, 4922 (1999); J. Garriga, O. Pujolas, and T. Tanaka, Nucl. Phys. **B605**, 192 (2001).

[15] C. Csaki, M. Graesser, L. Randall, and J. Terning, Phys. Rev. D **62**, 045015 (2000); C. Csaki, M. Graesser, and G. Kribs, Phys. Rev. D **63**, 065002 (2001).

[16] *Higher Transcendental Functions*, edited by A. Erdélyi (McGraw-Hill, New York, 1953), also known as "The Bateman Manuscript Project"; M. Abramowitz and I. A. Stegun, *Handbook of Mathematical Functions with Formulas, Graphs, and Mathematical Tables*, National Bureau of Standards, Applied Mathematics Series 55 (U.S. GPO, Washington, DC, 1972).

[17] K. Heun, *Zur Theorie der Riemann'schen Functionen Zweiter Ordnung mit vier Verzweigungspunkten*, Mathematische Annalen 33 (1889), pp. 161–179 (available at http://www.digizeitschriften.de/main/dms/img/#navi).

[18] A. Ronveaux, *Heun's differential equations* (Oxford University Press, New York, 1995).

[19] M. N. Hounkonnou and A. Ronveaux, Appl. Math. Comput. **209**, 421 (2009).

[20] E. S. Cleb-Terrab, J. Phys. A **37**, 9923 (2004).

[21] P. P. Fiziev, J. Phys. A **43**, 035203 (2010).